arXiv:cond-mat/9807041v2 [cond-mat.mes-hall] 21 Sep 1999

Magnetic-field-dependent zero-bias diffusive anomaly in Pb oxide-n-InAs structures: Coexistence of two- and three-dimensional states

G. M. Minkov[†], A. V. Germanenko, S. A. Negachev, O. E. Rut
Institute of Physics and Applied Mathematics,
Ural University, Ekaterinburg 620083, Russia

Eugene V. Sukhorukov[*‡]
Department of Physics and Astronomy, University of Basel,
Klingelbergstrasse 82, CH–4056 Basel, Switzerland
(February 1, 2008)

The results of experimental and theoretical studies of zero-bias anomaly (ZBA) in the Pb-oxide-n-InAs tunnel structures in magnetic field up to 6T are presented. A specific feature of the structures is a coexistence of the 2D and 3D states at the Fermi energy near the semiconductor surface. The dependence of the measured ZBA amplitude on the strength and orientation of the applied magnetic field is in agreement with the proposed theoretical model. According to this model, electrons tunnel into 2D states, and move diffusively in the 2D layer, whereas the main contribution to the screening comes from 3D electrons.

PACS numbers: 73.40.Gk, 73.23.Hk, 71.10.Pm, 73.20.-r

I. INTRODUCTION

It is well known that the electron-electron interaction strongly influences the transport properties of disordered conductors.[1] Even in the presence of weak disorder ($\varepsilon_F\tau_p \gg 1$, where ε_F is the Fermi energy, τ_p is the momentum relaxation time, and $\hbar = 1$) the electron-electron interaction suppresses the one-particle density of states at the Fermi level (diffusive anomaly). This leads to small deviations from Ohm's law in the current-voltage characteristics of a tunnel junction at small voltages V. The diffusive anomaly, which appears as a dip in the differential tunneling conductance $G = dI/dV$ at zero bias, reveals itself in almost all tunneling experiments and has been studied in various tunneling structures.[2] This should be distinguished from other nonlinearities of the current-voltage characteristics at low bias, which are due to different physical phenomena. The form of the diffusive zero-bias anomaly (ZBA) depends on the dimensionality: $\delta G(V) \propto \ln|V|$ for tunneling into two-dimensional (2D) conductors, and $\delta G(V) \propto \sqrt{|V|}$ for three-dimensional (3D) conductors. The width of the dip in the tunneling conductance is of order τ_p^{-1}, and therefore cannot be observed in pure conductors.

The first theoretical explanation of the diffusive ZBA, by Altshuler, Aronov and Lee in Refs. 3 and 4, was based on the diagrammatic perturbative method. For low-dimensional systems, this theory was subsequently extended beyond the perturbative treatment by Nazarov in Refs. 5 and 6 (see also Refs. 7,8, where the realistic system is described by the coupling of the tunnel junction with the effective electromagnetic environment), and later, by Levitov and Shytov in Ref. 9. Nazarov also gave a transparent physical interpretation of the diffusive ZBA; immediately after an electron tunnels into the diffusive conductor and forms the distribution $\rho(\mathbf{r},t)$, the system acquires an extra energy due to the interaction between this electron and the electrons in the conductor (Coulomb barrier). Therefore, the electron density perturbation $\rho(\mathbf{r},t)$ must spread under the Coulomb barrier in order to reach the final state. This process contributes a many-electron action $S(t)$ ($t \sim 1/eV$ is the time of spreading of the electron density perturbation) to the total tunneling action, and thereby, suppresses the tunneling current. In the regime of the Coulomb blockade effect ($S(t) \gg 1$) the tunneling current is almost completely suppressed. Conversely, in good metals ($\varepsilon_F\tau_p \gg 1$) the Coulomb interaction is screened, so that the many-electron action is small, $S(t) \ll 1$, and gives only small correction to the differential conductance. At $T = 0$, this takes the form

$$\frac{1}{G}\frac{dG}{dV} = \frac{2e}{\pi} Im\left\{ S(\omega)|_{i\omega\to -eV+i0}\right\} . \qquad (1.1)$$

The density of the tunneling electron $\rho_\omega(\mathbf{r})$ is given by a diffusion propagator (diffuson), whereas the electrodynamical potential $\phi_\omega(\mathbf{r})$ which it excites is given by

$$\phi_\omega(\mathbf{r}) = \int d\mathbf{r}' V_\omega(\mathbf{r},\mathbf{r}')\rho_\omega(\mathbf{r}'), \qquad (1.2)$$

where $V_\omega(\mathbf{r},\mathbf{r}')$ is the dynamically screened Coulomb potential. The action $S(\omega)$ is then explicitly given by:[5]

$$S(\omega) = \frac{1}{2}\int d\mathbf{r}\ \rho_{-\omega}(\mathbf{r})\phi_\omega(\mathbf{r}). \qquad (1.3)$$

This simple formula for the action displays an important role for the interface of the tunnel junction in the

ZBA in the case of tunneling into a 3D conductor. Indeed, after the electron tunnels through the barrier, it first appears on the surface of the conductor before propagating into the bulk. The surface of the conductor obviously affects the spreading process of the electron density ρ_ω. Consequently, it affects the amplitude of the ZBA. For example, it can partially block the spreading of the electron into final state, giving rise to additional factor of 2 in the amplitude of the anomaly[10] (the electron propagates into the half space). This interface effect is even more pronounced in the presence of a magnetic field. The role of the magnetic field is twofold. It causes the Lorentz force, which blocks the spreading of the electron density, but it also induces a Hall voltage, which causes a drift along the interface, and thereby enhances the spreading. If the magnetic field $\mathbf{B}$ is perpendicular to the junction interface, only the first effect contributes to the ZBA and gives a B^2 dependence of the ZBA.[4] If the magnetic field is parallel to the junction interface, the two effects exactly cancel. This results in the strongly anisotropic magnetic field dependence of the ZBA predicted in Ref. 11. Namely, the ZBA depends only on the component of the magnetic field perpendicular to the interface of the junction, as it would be in the case of tunneling into a 2D conductor. This effect has probably been observed in Refs. 12 and 13.

Motivated by this physical situation, we theoretically and experimentally investigated the ZBA in Pb-oxide-n-InAs structures in the presence of a magnetic field. We expected that the specific feature of these structures, namely, coexistence of 3D and 2D electron states near the surface of InAs, will strongly influence the ZBA and especially its magnetic field dependence. In particular, as the current in these structures can occur through the tunneling of electrons into both 2D and 3D states, the principle question which arises is whether the ZBA has 2D or 3D character. The results of our study can be summarized as follows. The electrons tunnel into 2D states and move diffusively in a 2D layer, whereas the main contribution to the screening comes from 3D electrons. This gives rise to the unusual magnetic field dependence of the ZBA. When the magnetic field $\mathbf{B}$ is perpendicular to the interface of the tunnel junction, the amplitude of the ZBA grows as B^2 in agreement with Ref. 4. The ZBA amplitude strongly depends on the orientation of the magnetic field, in agreement with Ref. 11. However, when the magnetic field lies in the plane of the junction interface, the magnetic field dependence does not disappear. Instead, the ZBA amplitude is linear in B.

II. EXPERIMENTAL RESULTS

The differential conductance $G = dI/dV$ and its derivative (dG/dV) as a function of bias and magnetic field in Pb-oxide-n-InAs tunnel structures were investigated in a magnetic field up to 6 T at temperatures 4.2

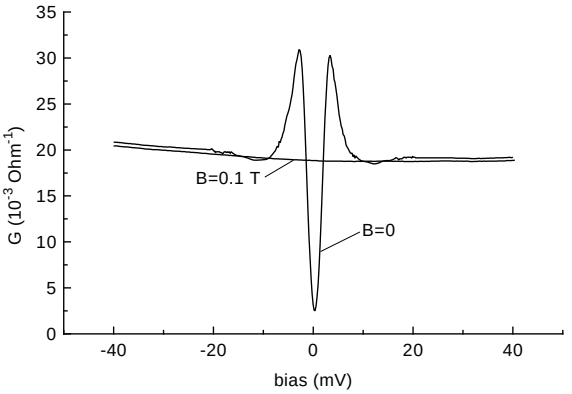

FIG. 1. Bias dependencies of the differential conductance G for structure 1 at T= 1.6 K.

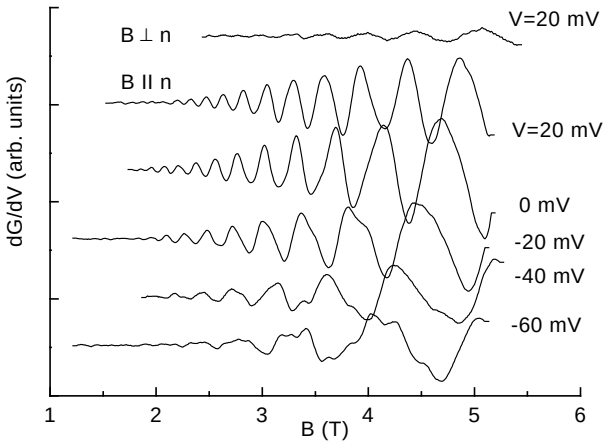

FIG. 2. Magnetic field dependence of dG/dV for different biases. The topmost curve is for $\mathbf{B} \perp \mathbf{n}$, and the others are for $\mathbf{B} \parallel \mathbf{n}$ (structure 1). All curves are at T= 4.2 K.

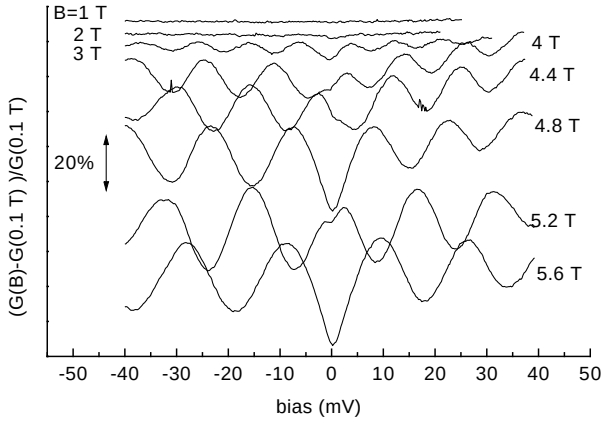

FIG. 3. Bias dependencies of $(G(B) - G(0.1T))/G(V, 0.1T)$ for different magnetic fields $\mathbf{B} \parallel \mathbf{n}$ at T= 4.2 K.

and 1.6 K. The tunnel structures were fabricated on n-InAs wafers with two different pairs of electron concentration and mobility: 9.7×10^{17} cm^{-3}, and 1.5×10^4 $cm^2V^{-1}s^{-1}$ (structure 1); and 1.9×10^{17} cm^{-3}, and 1.8×10^4 $cm^2V^{-1}s^{-1}$ (structure 2). Ultraviolet illumination for 10–15 min in dry air was used to form the thin oxide, which served as a tunneling barrier. The Pb electrode was then evaporated through a mask. The tunnel contacts fabricated on each wafer were similar and results are shown for one of several contacts fabricated on each wafer. The traditional modulation procedure was used for measuring the differential conductance and its derivative. Measurements showed that decreasing of the modulation amplitudes below 0.2 mV do not change the features in the G *vs.* V curves. Therefore, in all investigations the modulation amplitude was 0.2 mV.

The dominant contribution to the current in the investigated structure is a tunneling current. This is evident from the bias dependencies of the differential conductance, which are shown on Fig. 1. The structure of the curve for $B = 0$ is the "superconducting anomaly", connected with the superconducting gap in the one particle density of states in the metal electrode. At $B > 0.06$ T the superconductivity of Pb is destroyed and this structure disappears completely.

Oscillations in G and dG/dV as a function of V and B were observed for both $\mathbf{B} \parallel \mathbf{n}$ and $\mathbf{B} \perp \mathbf{n}$, where $\mathbf{n}$ is the normal to the plane of the tunnel junction (Figs. 2 and 3). The tunneling conductance oscillations in such types of structures were comprehensively studied in InAs,[14–16] and in HgCdTe.[17,18] It was shown that in the structures based on InAs, an accumulation layer with 2D subbands exists near the barrier (Fig. 4). The tunneling conductance is determined by tunneling into both 3D and 2D states of the semiconductor electrode. Having $\mathbf{B} \parallel \mathbf{n}$ leads to quantization of the spectrum of both 2D and 3D states. For this orientation of the magnetic field, the oscillations in G are mainly due to the modulation of the density of 2D states. Having $\mathbf{B} \perp \mathbf{n}$ does not quantize the energy spectrum of 2D states and the oscillations in G are only due to tunneling into 3D states. At fixed bias V, these oscillations are periodic in $1/B$. Therefore, using the Fourier transformation one can determine the fundamental fields B_f and, consequently, the quasi-momenta $k = \sqrt{2eB_f/c\hbar}$ of 2D and bulk states at the energy $\varepsilon_F + eV$. In addition, such data processing allows us to determine the energies of the bottoms of the conduction band and 2D subbands counted from the Fermi energy of the semiconductor (for more details, see Refs. 14 and 17). Thus, we found that in structure 1 there are bulk states with $\varepsilon_F - \varepsilon_c = 115$ meV and $k_b^2(\varepsilon_F) = 9.3 \times 10^{12}$ cm^{-2}, states of the ground 2D subband with $\varepsilon_F - \varepsilon^0 \simeq 160$ meV and $k_0^2(\varepsilon_F) = 20.6 \times 10^{12}$ cm^{-2}, and states of the excited 2D subband with $\varepsilon_F - \varepsilon^1 \simeq 120$ meV and $k_1^2(\varepsilon_F) = 10.3 \times 10^{12}$ cm^{-2}. For the structure 2 these parameters are $\varepsilon_F - \varepsilon_c = 50$ meV and $k_b^2(\varepsilon_F) = 3.1 \times 10^{12}$, $\varepsilon_F - \varepsilon^0 \simeq 95$ meV and $k_0^2(\varepsilon_F) = 7.6 \times 10^{12}$, and $\varepsilon_F - \varepsilon^1 \simeq 55$ meV and $k_1^2(\varepsilon_F) = 3.5 \times 10^{12}$ cm^{-2}.

Now let us consider G *vs.* V curves in the vicinity of zero bias. The relative difference $(G(V,B) - G(V,0.1\text{ T}))/\,G(V,0.1\text{ T})$ as a function of voltage for various magnetic fields $\mathbf{B} \parallel \mathbf{n}$ is presented in Fig. 3. It is seen that increasing B gives rise to a dip in the conductance in the vicinity of $V = 0$, which is better seen when it falls between adjacent 2D Landau levels. This peculiarity is more pronounced in $\Delta\,(dG(V,B)/dV) = dG(V,B)/dV - dG(V,0.1\text{ T})/dV$ *vs.* V curves (Fig. 5a). To separate out the ZBA from the conductance oscillations (due to Landau quantization), the following procedure was used; after taking the Fourier transformation (Fig. 5b) we cut out the components associated with the oscillations and then take the inverse Fourier transformation (Fig. 5c). Such a procedure greatly helps in extracting the anomaly from the oscillations, but does not completely separate the ZBA from the oscillations. Therefore, we cut out the part of the curve in the range ± 5 mV in vicinity of $V = 0$ (Fig. 5c), interpolate the rest of the curve by a smooth line, and then subtract this line from the initial curve shown in Fig. 5c. After integration, we obtain the ZBA in the tunneling conductance (Fig. 5d). (The correctness of such processing was verified by separating out the Gaussian shape from the simulating curve $A_1 \sin(\omega_1 V + \varphi_1) + A_2 \sin(\omega_2 V + \varphi_2) + A_3 \exp(-(V/\Delta)^2$.)

The magnetic field dependencies of the normalized amplitude $A = -\delta G/G|_{V=0}$ and halfwidth of the ZBA are plotted in Fig. 6. It is seen that the halfwidth does not vary with the magnetic field within the experimental error, whereas the amplitude of the ZBA significantly increases. The inset in Fig. 6a shows that the A *vs.* B dependence is close to $A \propto B^2$. Similar results are obtained for the structure 2 (Fig. 7). In addition, one can see an oscillatory dependence of A on B, which appears at high magnetic fields. The minima of the oscillations are observed at those magnetic fields where the 2D Landau levels cross the Fermi level. Thus, the origin of the oscillations of the ZBA amplitude is the Landau quantization of electron states in the 2D layer. The detailed investigation of this effect will be the subject of future work. Therefore, we will not concentrate on these oscillations in this paper.

The angular dependence of the ZBA amplitude is plotted in Fig. 8 (φ is the angle between $\mathbf{B}$ and $\mathbf{n}$). One can see that the ZBA amplitude is strongly anisotropic. It drastically decreases when the magnetic field deviates from $\mathbf{B} \parallel \mathbf{n}$, but it does not disappear at $\mathbf{B} \perp \mathbf{n}$. The magnetic field dependence of the ZBA amplitude for this orientation is significantly weaker and is close to linear (Fig. 7).

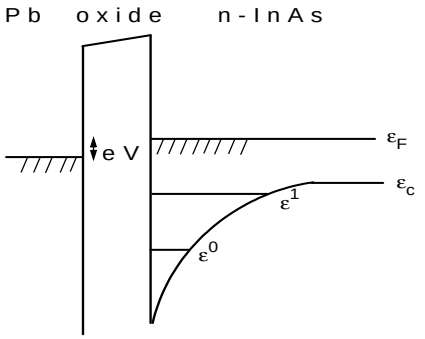

FIG. 4. Energy diagram of the Pb-oxide-n-InAs tunnel structure. ε^0 and ε^1 are the energies of the bottom of the ground and excited 2D subbands respectively, and ε_c is the energy of the bottom of the conduction band.

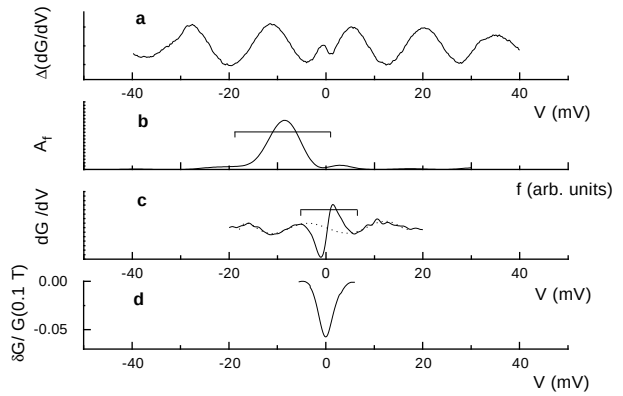

FIG. 5. (a) The bias dependence of $\Delta(dG(V,B)/dV) = dG(V,B)/dV - dG(V,0.1\text{ T})/dV$ for $B = 5.3$ T and $\mathbf{B} \parallel \mathbf{n}$. (b) Fourier transform of the upper curve. The bar shows the region which was cut out. (c) Result of inverse Fourier transform. The dotted curve is the interpolation after the central region was cut out. (d) Reconstructed zero-bias anomaly after the processing described in the text.

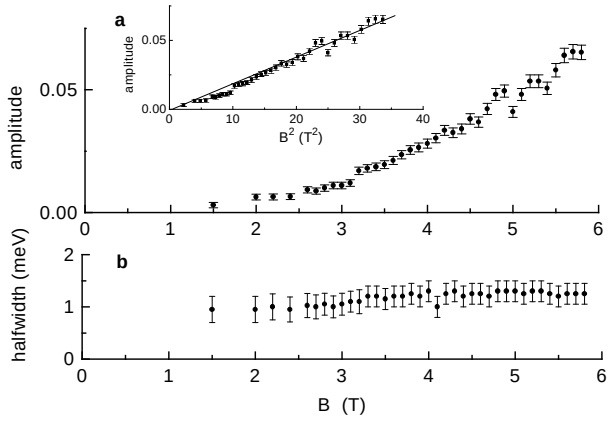

FIG. 6. Magnetic field dependencies of the amplitude (a) and halfwidth (b) of the ZBA, for $\mathbf{B} \parallel \mathbf{n}$. The inset shows the A *vs.* B^2 dependence. All points are at T= 4.2 K.

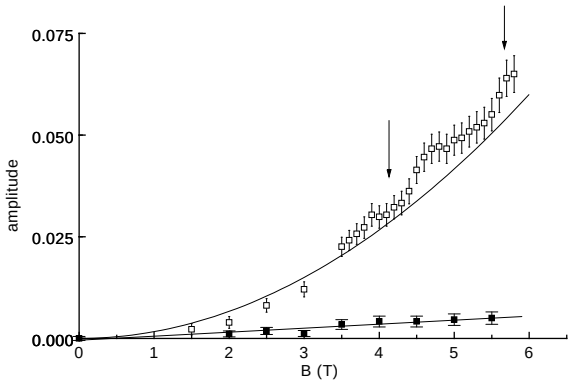

FIG. 7. Magnetic field dependencies of the ZBA amplitude for $\mathbf{B} \parallel \mathbf{n}$ (open squares) and $\mathbf{B} \perp \mathbf{n}$ (full squares) for structure 2 at T= 4.2 K. The arrows indicate the magnetic fields, for which the 2D Landau levels coincide with the Fermi level.

III. DISCUSSION

The energy scale of the diffusive anomaly caused by electron-electron interaction in dirty conductors is τ_p^{-1}. In our structures, τ_p^{-1} is estimated from the mobility to be about 2 meV, whereas the halfwidth of the ZBA is 1 meV (Fig. 6b). Thus, we suppose that the ZBA observed in our experiment is just the diffusive anomaly. The specific feature of the investigated structures is the coexistence of 2D and 3D electrons near the barrier. Therefore the basic question is whether the zero-bias anomaly is due to the interaction of 2D or 3D electrons. In principle, the ZBA has different form for tunneling into 2D and 3D states: $\delta G(V) \propto ln|V|$ for 2D and $\delta G(V) \propto \sqrt{|V|}$ for 3D. However, the comparison of fits to experimental data in Fig. 9 does not allow us to distinguish between the two forms of the ZBA.

On one hand, the main part of the tunneling conductance is due to tunneling into the 2D states. This follows from the theoretical calculation of the tunneling conductance for the investigated structures carried out in the framework of the transfer Hamiltonian method.[19] Such a calculation shows that the tunneling conductance due to tunneling into the 2D states is larger by about a factor of 5 than that for tunneling into 3D states. This conclusion is also supported by the fact that the amplitude of oscillations of the tunneling conductance caused by the Landau quantization is significantly larger in the case of tunneling into 2D states (at $\mathbf{B} \parallel \mathbf{n}$) than in the case of tunneling into 3D states ($\mathbf{B} \perp \mathbf{n}$) (Fig. 2). In addition, the ZBA amplitude has typical for 2D systems strong dependence on the magnetic field orientation, i.e. it is determined mainly by the normal component of the magnetic field (Fig. 8). Therefore, one can surmise that the ZBA has 2D character.

On the other hand, the strong angular dependence of the ZBA is ambiguous evidence of the 2D nature of the ZBA. Indeed, in Ref. 11 it was demonstrated that for

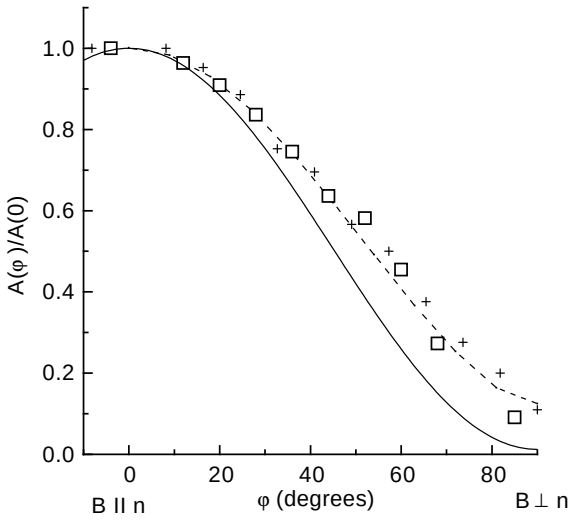

FIG. 8. Angular dependence of the ZBA amplitude, for B=5.5 T. The crosses and squares are data for structures 1 and 2 respectively. The dashed curve is the result of the calculation described in the text. The solid curve corresponds to the 3D case.

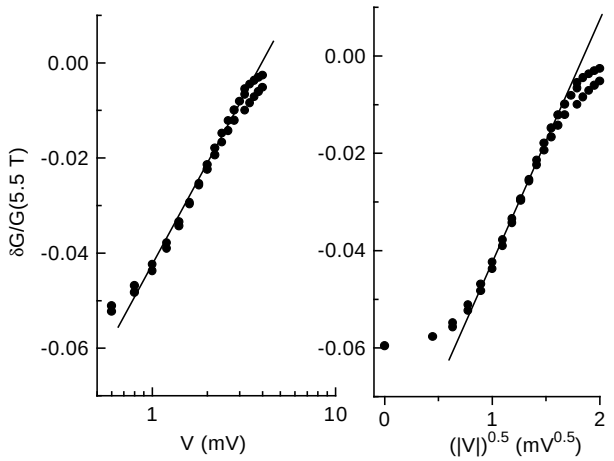

FIG. 9. Tunneling conductance near $V = 0$ versus $\ln|V|$ (a) and versus $|V|^{0.5}$ (b) at T= 1.6 K, B=5.5 T The two sets of data points correspond to different signs of the bias.

tunneling into 3D states the amplitude of the ZBA is given by $A(B) \propto 1 + \omega_c^2\tau_p^2\cos^2(\varphi)$ (where ω_c is cyclotron frequency), i.e. it depends only on the component of the magnetic field perpendicular to the interface of the junction, as it would be in the case of tunneling into a 2D conductor. In the limit $\omega_c^2\tau_p^2 \gg 1$ this leads to the strong angular dependence of the ZBA amplitude. Although the strong anisotropy of the ZBA is observed in our experiment for $\omega_c^2\tau_p^2 \simeq 50$ at $B = 5.5$ T, the curve $1 + \omega_c^2\tau_p^2\cos^2(\varphi)$ does not fit well with the experimental data (see the Fig. 8). Moreover, the ZBA amplitude is linear in B when the magnetic field lies in the plane of the junction interface (see Fig. 6).

Thus, the magnetic field dependence of the ZBA in the investigated structures does not completely agree with either the 3D or 2D nature of the ZBA. We would like to stress however, that our experimental set up is not usual for studying the diffusive ZBA. Traditionally, the 2D metallic layer in tunnel junctions is electrically isolated from the 3D electrode (or another 2D layer). In this case the charge relaxation is two-dimensional and the interaction is partially screened by the 3D metal, so that its strength is defined by the distance Δ between 2D and 3D electrodes. The correction to the differential conductance then has the form[10] $\delta G(V) \sim \ln(a\Delta/r_D^2)\ln(eV\tau_p)$, where a is the width of the 2D layer, and r_D is the Debye radius. In addition, it is assumed that this formula holds for $a\Delta/r_D^2 \gg 1$ and $\Delta/r_D \gg 1$. Thus, there are two reasons which make our experimental set up different from the usual one, and the above formula nonapplicable to our case. The specific feature of the investigated structures is coexistence of 3D and 2D electron states near the surface of the semiconductor (see Fig. 4). Thus, formally in our case $\Delta = 0$. Second, and this is most important, in our experiment the 2D electron system and 3D metal are not electrically isolated.

In the next section we show that the following scenario of tunneling is realized in this structures. After tunneling, the electron moves diffusively in the 2D layer and forms the 2D distribution $\rho_\omega(\mathbf{r})$ at the surface of the semiconductor. It immediately pushes other electrons into the bulk, so that the total charge becomes zero for a short time of order of the inverse plasma frequency. Thus, the relaxation of the *total* charge takes three-dimensional form, and this should lead to $\sqrt{V}$-dependence of the differential conductance usual for the 3D ZBA. The dimensionality of $\rho_\omega(\mathbf{r})$ does not affect the voltage dependence of the differential conductance. However, it leads to the unusual magnetic field dependence of the ZBA discussed above.

IV. THEORETICAL MODEL AND COMPARISON WITH EXPERIMENTAL DATA

In our theoretical analysis we make two assumptions. First, we assume that the probability of electrons tunneling into 2D states near the surface of the semiconductor is much greater than the probability of tunneling into 3D bulk states. This follows from the analysis of the experimental results in the previous sections. The second assumption is that the tunneling electron (though being screened by the other electrons of the system) remains in the 2D well for a physically relevant time, i.e. for the time $t \sim 1/eV$ (see discussion in Sec. I) before escaping into the bulk. This last time ranges from τ_p to $(kT)^{-1}$ in the ZBA regime, and thus in our experiment it may exceed the momentum relaxation time by factor of 10. On the other hand, the escape of electrons from the 2D

well to the bulk is determined by the ionized impurity scattering, which is main scattering mechanism at low temperatures. This mechanism is strongly anisotropic – the small angle scattering dominates. Together with requirement of large momentum transfer for 2D→3D transition this leads to the fact that the 2D → 2D transition rate $W_{22} \sim (\tau_p)^{-1}$ is larger than the 2D → 3D transition rate, W_{23}. The calculations with wave functions and screening radius corresponding to the investigated structures carried out in the same manner as in Ref. 20 gives $W_{22}/W_{23} \approx 15$. Thus, the second assumption is justified.

The width of the 2D well is of order λ_F and is much smaller than the mean free path l_3 in the bulk of the conductor. Therefore, the 2D well can be thought of as a δ-layer with respect to the physically relevant length scale. This means that after tunneling the electron forms a 2D density distribution $\rho_\omega(\mathbf{r}) = Q_\omega(\mathbf{R})\delta(z)$ localized on the surface $z = 0$ of the conductor (here, $\mathbf{R} = (x, y)$ is the coordinate on the surface, and $\mathbf{r} = (\mathbf{R}, z)$). Then, due to the interaction of this electron with the ones forming both 2D and 3D liquids, the electrodynamic potential ϕ_ω is excited.

Instead of a direct calculation of the integral (1.2) for ϕ_ω, we follow Ref. 11 and use the electroneutrality principle. We assume that the density of the tunneling electron is completely screened on the distance of the order of Debye radius r_D, so that the induced charge density is $\tilde{\rho}_\omega(\mathbf{r}) = -\rho_\omega(\mathbf{r}) = -Q_\omega(\mathbf{R})\delta(z)$. Taking into account charging effects[11] gives only corrections of order $r_D^2/wl_3 \ll 1$ (w is the thickness of the tunneling barrier), which we neglect here. We also assume that the Pb electrode, being a good metal, does not contribute to the action $S(\omega)$. Therefore, after Fourier transformation the integral (1.3) can be represented in the following form:

$$S(\omega) = \frac{1}{8\pi^2} \int d\mathbf{k}\, Q_{-\omega}(-\mathbf{k})\Phi_\omega(\mathbf{k}), \tag{4.1}$$

where $\Phi_\omega(\mathbf{k}) = \phi_\omega(\mathbf{k}, z)|_{z=0}$.

The density Q_ω obeys the 2D diffusion equation in imaginary time

$$|\omega|Q_\omega - D_2\nabla^2_{\mathbf{R}}Q_\omega = -e\, sign(\omega)\delta(\mathbf{R} - \mathbf{R}_0), \tag{4.2}$$

with the diffusion coefficient $D_2 \equiv D_2(\mathbf{B})$, which depends only on the z-component of the magnetic field $\mathbf{B} = (B, \varphi)$:

$$D_2(\mathbf{B}) = \frac{D_2^{(0)}}{1 + \omega_c^2\tau_2^2\cos^2\varphi}. \tag{4.3}$$

Here, ω_c is the cyclotron frequency and $D_2^{(0)} \equiv D_2(0)$. We have introduced the new notation, τ_2, for the momentum relaxation time of 2D electrons to distinguish it from that of 3D electrons. After Fourier transformation, equation (4.2) can be immediately solved,

$$Q_\omega(\mathbf{k}) = -\frac{e\, sign(\omega)}{|\omega| + D_2\mathbf{k}^2}. \tag{4.4}$$

To calculate the potential Φ_ω we formulate and then solve the system of equations for the dynamics of the induced charge density $\tilde{\rho}_\omega = -Q_\omega\delta(z)$. This dynamics is controlled by the transport along the 2D layer, as well as by the nonzero current perpendicular to the layer $j_n(\omega, \mathbf{R})$. The conservation of charge (in imaginary time) reads,

$$|\omega|Q_\omega - D_2\nabla^2_{\mathbf{R}}Q_\omega + \sigma_2\nabla^2_{\mathbf{R}}\Phi_\omega = j_n, \tag{4.5}$$

where we introduced the 2D conductivity $\sigma_2(\mathbf{B}) = e^2\nu_2 D_2(\mathbf{B})$, and ν_2 is the Fermi density of 2D states. On the left hand side of this equation the second and third terms are the divergences of the diffusion and electrical currents respectively. The first two terms of this equation coincide with the left-hand side of Eq. (4.2) for the diffusion propagator Q_ω. This is precisely the reason for the cancellation of the diffusion pole discussed below. Now, we can use this fact to eliminate Q_ω from the last equation:

$$j_n - \sigma_2\nabla^2_{\mathbf{R}}\Phi_\omega = -e\, sign(\omega)\delta(\mathbf{R} - \mathbf{R}_0). \tag{4.6}$$

On the other hand, in the bulk of the conductor the charge is not accumulated, $\tilde{\rho}_\omega|_{z>0} = 0$. The conservation of charge then leads to $\nabla\mathbf{j}(\omega, \mathbf{r}) = 0$ and $\mathbf{n}\cdot\mathbf{j}(\omega, \mathbf{r})|_{z=0} = j_n(\omega, \mathbf{R})$, where $\mathbf{j}$ is the density of current in the bulk of the conductor. These two equations can be expressed in terms of ϕ_ω:

$$\nabla_{\mathbf{r}}\cdot\hat{\sigma}\nabla_{\mathbf{r}}\phi_\omega(\mathbf{R}, z) = 0, \tag{4.7}$$

$$\mathbf{n}\cdot\hat{\sigma}\nabla_{\mathbf{r}}\phi_\omega(\mathbf{R}, z)|_{z=0} = -j_n(\omega, \mathbf{R}), \tag{4.8}$$

where $\hat{\sigma} \equiv \hat{\sigma}(\mathbf{B})$ is the conductivity tensor in the bulk of the conductor. If the magnetic field is perpendicular to the surface of the conductor ($\varphi = 0$), the conductivity tensor takes the simple form:

$$\sigma_{xx} = \sigma_{yy} = \frac{\sigma_3^{(0)}}{1 + \omega_c^2\tau_3^2}, \quad \sigma_{zz} = \sigma_3^{(0)}\,, \tag{4.9}$$

$$\sigma_{xy} = -\sigma_{yx} = -sign(\omega)\,\frac{\sigma_3^{(0)}\omega_c\tau_3}{1 + \omega_c^2\tau_3^2}\,, \tag{4.10}$$

and all other elements vanish. Here, $\sigma_3^{(0)}$ is the conductivity of 3D electrons in the case of zero magnetic field, and τ_3 is the momentum relaxation time of 3D electrons. In the case of arbitrary magnetic field orientation, $\hat{\sigma}$ can be calculated by the rotation over the angle φ, $\hat{\sigma}(\mathbf{B}) = \hat{U}(-\varphi)\hat{\sigma}(\mathbf{B})|_{\varphi=0}\hat{U}(\varphi)$.

Solving Eqs. (4.6,4.7,4.8) simultaneously, we get,

$$\Phi_\omega(\mathbf{k}) = -\frac{e\, sign(\omega)}{\sigma_3^{(0)}Z + \sigma_2\mathbf{k}^2}, \tag{4.11}$$

where the function $Z(\mathbf{B}, \mathbf{k})$ is given by

$$Z(\mathbf{B}, \mathbf{k}) = \frac{\sqrt{k_x^2\cos^2\alpha + k_y^2} + ik_x\sin\alpha}{\sqrt{1 + \omega_c^2\tau_3^2}}, \tag{4.12}$$

with the angle α defined by

$$\frac{\sin\alpha}{\sin\varphi} = sign(\omega)\frac{\omega_c\tau_3}{\sqrt{1+\omega_c^2\tau_3^2}}. \quad (4.13)$$

Finally, we substitute Q_ω from (4.4) and Φ_ω from (4.11) into Eq. (4.1), and arrive at the following formula for the action:

$$S(\omega) = -\frac{e^2}{8\pi^2}\int \frac{d\mathbf{k}}{(|\omega| + D_2\mathbf{k}^2)\left(\sigma_3^{(0)}Z + \sigma_2\mathbf{k}^2\right)}. \quad (4.14)$$

We would like to mention the cancellation of the diffusion pole in the expressions (4.11) and (4.14) (compare to Eqs. (1.2,1.3)). This well known fact (see for example Ref. 1) physically means that after tunneling, the accommodation of the charge is entirely governed by plasmon modes.

In the equation (4.14) two terms in the denominator of the integrand, $\sigma_3^{(0)}Z$ and $\sigma_2\mathbf{k}^2$, are contributions from the screening of the tunneling electron by 3D and 2D electrons, respectively. In principle, one can expect to observe the crossover from 3D ZBA with $S(\omega) \sim 1/\sqrt{\omega}$ ($g = \sigma_3^{(0)}Z/\sigma_2\mathbf{k}^2 \gg 1$) to 2D ZBA with $S(\omega) \sim 1/\omega$ ($g \ll 1$). In our case, however, the screening by 2D electrons is weak. Indeed, the integral (4.14) should be evaluated for $\omega \sim 1/\tau_2$. For $\varphi = 0$, the simple estimate then gives $g \sim k_F l_3 \gg 1$ in the case of zero magnetic field, and $g \sim k_F l_2 \gg 1$ in strong magnetic field, $\omega_c\tau_{2,3} \gg 1$ (here, l_2 is the mean free path in the 2D layer). For $\varphi = \pi/2$ we have $g \sim \varepsilon_F/\omega_c \gg 1$ in strong magnetic field. Therefore, we can neglect screening by 2D electrons. This equally means that in Eq. (4.5), for the induced charge density Q_ω, we can neglect the 2D current, $-\sigma_2\nabla^2_{\mathbf{R}}\Phi_\omega$, compared to the 3D current, j_n (given by Eq. (4.8)). Thus, after tunneling the charge relaxation process has 3D character. This leads to a $\sqrt{V}$ dependence of the differential conductance, as is usual for 3D. We show this next.

Omitting the term $\sigma_2\mathbf{k}^2$ in the denominator in the right hand side of (4.14), we carry out the integration over $\mathbf{k}$ and obtain,

$$S(\omega) = -\frac{e^2}{4\pi\sigma_3^{(0)}\sqrt{|\omega|D_2^{(0)}}}F(B,\varphi), \quad (4.15)$$

$$F(B,\varphi) = \sqrt{(1+\omega_c^2\tau_3^2)\,(1+\omega_c^2\tau_2^2\cos^2\varphi)}E(\sin\alpha), \quad (4.16)$$

where $E(s) = \int_0^{\pi/2} d\theta\sqrt{1-s^2\sin^2\theta}$ is the complete elliptic integral. Substituting the action $S(\omega)$ from Eq. (4.15) into Eq. (1.1), we arrive at the final result,

$$\frac{1}{G}\frac{dG}{dV} = \frac{e^3}{2\pi^2\sigma_3^{(0)}\sqrt{2eVD_2^{(0)}}}F(B,\varphi). \quad (4.17)$$

The correction to the differential conductance then takes the form $\delta G \sim \sqrt{V}$.

Next we concentrate on the magnetic field dependence of the ZBA. The fact that the magnetic field and V dependencies of the differential conductance are completely factorized allows us to represent the normalized amplitude of the ZBA, $A(B,\varphi) \equiv -\delta G/G|_{V=0}$, in a simple form. To do this, we integrate Eq. (4.17) over V and cut the integral at $eV \sim \tau_2^{-1}$. We then arrive at the following result:

$$A(B,\varphi) = A_0F(B,\varphi), \quad (4.18)$$

where $A_0 = \kappa\lambda_F^2/l_2l_3$, and κ is a dimensionless number of order 1. The equation (4.18), together with Eq. (4.16), represents the general result which is valid for an arbitrary magnetic field. Now we consider the most interesting case of strong magnetic field, $\omega_c\tau_3 \gg 1$. In this limit $\sin^2\alpha = \sin^2\varphi$ and introducing the dimensionless parameter $h = \omega_c\tau_2$ we can write,

$$A(B,\varphi) = \kappa\left(\lambda_F/l_2\right)^2 h\sqrt{1+h^2\cos^2\varphi}E(\sin\varphi). \quad (4.19)$$

We are now in a position to compare the result of our theoretical analysis with the experimental data. When the magnetic field is perpendicular to the interface of the tunnel junction, $\varphi = 0$, we have ($\omega_c\tau_2 \gg 1$):

$$A(B,0) = \frac{\pi\kappa}{2}\left(\frac{\lambda_F h}{l_2}\right)^2 = \frac{\pi\kappa}{2}\left(\frac{\lambda_F}{R_c}\right)^2, \quad (4.20)$$

where R_c is the cyclotron radius. The amplitude of the anomaly thus goes as B^2. As it is clearly seen from Figs. 6 and 7, the experimental data for $\mathbf{B} \parallel \mathbf{n}$ are close to this dependence for both structures. Remarkably, the amplitude of the anomaly does not depend on τ_2 and τ_3 (see Eq. (4.20)). However, contrary to one's first expectation, the ZBA cannot be observed in a perfect 3D metal. Although the amplitude of the anomaly stays constant with $\tau_{2,3} \to \infty$, the dip of the tunneling conductance gets narrower (its width is given by τ_2^{-1}) and finally shrinks.

When the magnetic field is parallel to the junction interface, $\varphi = \pi/2$, from Eq. (4.19) we obtain,

$$A(B,\pi/2) = \kappa\left(\frac{\lambda_F}{l_2}\right)^2 h, \quad (4.21)$$

i.e. the amplitude of ZBA is a linear function of magnetic field. The same dependence is observed experimentally (see Fig. 7).

Finally, we can keep the amplitude of the magnetic field constant and study the angular dependence of the ZBA. From Eq. (4.19) it follows that

$$\frac{A(B,\varphi)}{A(B,0)} = \frac{2}{\pi h}\sqrt{1+h^2\cos^2\varphi}E(\sin\varphi). \quad (4.22)$$

This dependence and the dependence corresponding to the pure 3D case[11] are plotted in Fig. 8. One can see that the expression (4.22) is in excellent agreement with the experimental data without any fitting parameters.

V. CONCLUSION

We have presented the results of experimental and theoretical studies of the zero-bias anomaly (ZBA) in tunnel structures with 2D and 3D electron states coexisting near the semiconductor surface. It has been shown that the specific scenario of tunneling realized in this structures is: (i) electrons tunnel mainly into 2D states, (ii) immediately after tunneling, the electrons move diffusively in a 2D layer, and (iii) the main contribution to screening comes from the 3D electrons and, as a result, the charge relaxation has a 3D character.

This leads to the peculiar features of the magnetic field dependence of the ZBA amplitude. When the magnetic field is perpendicular to the interface of the tunnel junction, the ZBA amplitude grows as B^2, in agreement with Ref. 4. Although the magnetic field dependence has strong anisotropy, as predicted in Ref. 11, it does not disappear completely when the magnetic field lies in the plane of the junction interface. Instead, the ZBA amplitude is linear in B.

The experimental data show that the ZBA amplitude oscillates with the magnetic field. The origin of the oscillations is the Landau quantization of electron states in the 2D layer. The detailed investigation of this effect will be the subject of future work.

ACKNOWLEDGMENTS

We would like to thank J. Kyriakidis for a critical reading of the manuscript and for very helpful discussion. This work was supported in part by the RFBR through Grants 97-02-16168 and 98-02-17286, the Russian Program *Physics of Solid State Nanostructures* through Grant 97-1091, and the Program *University of Russia* through Grant 420 at the Institute of Physics and Applied Mathematics, and by the Swiss National Science Foundation at the University of Basel (E.V.S.)

---

† email: Grigori.Minkov@usu.ru

* email: sukhorukov@ubaclu.unibas.ch

‡ On leave from Institute of Microelectronics Technology, Russian Academy of Sciences, Chernogolovka, 142432 Russia.

[1] B. L. Altshuler, and A. G. Aronov, in *Electron-Electron Interaction in Disordered Systems*, edited by A. L. Efros, and M. Pollak (Elsevier, Amsterdam, 1985).

[2] V. N. Lutskii, A. S. Rylik, and A. K. Savchenko, Pis'ma Zh. Exsp. Teor. Fiz. **41**, 134 (1985) [JETP Lett. **41**, 163 (1985)]; Alice E. White, R. C. Dynes, and J. P. Garno, Phys. Rev. B**31**, 1174 (1985); M. E. Gershenzon, V. N. Gubankov, and M. I. Falei, Zh. Eksp. Teor. Fiz. **90**, 2196 (1986) [Sov. Phys. JETP **63**, 1287 (1986)]; J. M. Valles, Jr., R. C. Dynes, and J. P. Garno, Phys. Rev. B**40**, 7590 (1989); P. Delsing, K. K. Likharev, L. S. Kuzmin, and T. Claeson, Phys. Rev. Lett. **63**, 1180 (1989); R. C. Ashoori, J. A. Lebens, N. P. Bigelov, and R. H. Silsbee, Phys. Rev. B**48**, 4616 (1993); Shih-Ying Hsu and J. M. Valles, Jr., Phys. Rev. B**49**, 16600 (1994); J. P. Kauppinen and J. P. Pekola, Phys. Rev. Lett. **77**, 3889 (1996); D. N. Davidov, J. Haruyama, D. Routkevitch, B. V. Statt, M. Moskovits, and J. M. Xu, Phys. Rev. B**57**, 13550 (1998); T. A. Polyanskaya, T. Yu. Allen, Kh. G. Nazhmudinov, and I. G. Savel'ev, Semiconductors, **32**, 517 (1998). For the review of early experiments, see E. L. Wolf, *Principles of Electron Tunneling Spectroscopy* (Clarendon Press, Oxford, 1985).

[3] B. L. Altshuler and A. G. Aronov, Solid State Commun. **30**, 115 (1979); B. L. Altshuler, A. G. Aronov and P. A. Lee, Phys. Rev. Lett. **44**, 1288 (1980).

[4] B. L. Altshuler, and A. G. Aronov, Zh. Eksp. Teor. Fiz. **77**, 2028 (1979) [Sov. Phys. JETP **50**, 968 (1979)].

[5] Yu. V. Nazarov, Zh. Eksp. Teor. Fiz. **95**, 975 (1989) [Sov. Phys. JETP **68**, 561 (1989)].

[6] Yu. V. Nazarov, Fiz. Tverd. Tela **31**, 188 (1989) [Sov. Phys. Solid State **31**, 1581 (1989)].

[7] M. H. Devoret, D. Esteve, H. Grabert, G.-L. Ingold, H. Pothier, and C. Urbina, Phys. Rev. Lett. **64**, 1824 (1990).

[8] G.-L. Ingold, and Yu. V. Nazarov, in *Single Charge Tunneling*, edited by H. Grabert and M. H. Devoret (Plenum, New York, 1992).

[9] L. S. Levitov, and A. V. Shytov, Pis'ma Zh. Eksp. Teor. Fiz. **66**, 200 (1997) [Sov. Phys. JETP Lett. **66**, 214 (1997)].

[10] B. L. Altshuler, A. G. Aronov, and A. Yu. Zuzin, Zh. Eksp. Teor. Fiz. **86**, 709 (1984) [Sov. Phys. JETP **59**, 415 (1984)].

[11] E. V. Sukhorukov and A. V. Khaetskii, Phys. Rev. B**56**, 1456 (1997).

[12] I. N. Kotel'nikov, A. S. Rylik, and A. Ya. Shul'man, Pis'ma Zh. Eksp. Teor. Fiz. **58**, 831 (1993) [Sov. Phys. JETP Lett. **58**, 779 (1993)].

[13] Yu. V. Dubrovskii, Yu. N. Khanin, T. G. Andersson, U. Gennser, D. K. Maude, and J.-C. Portal, Zh. Eksp. Teor. Fiz. **109**, 868 (1996) [Sov. Phys. JETP **82**, 467 (1996)].

[14] D. C. Tsui, Phys. Rev. B**8**, 2657 (1973).

[15] D. C. Tsui, Phys. Rev. B**12**, 5739 (1975).

[16] D. C. Tsui, Phys. Rev. B**12**, 5853 (1975).

[17] G. M. Minkov, A. V. Germanenko, V. A. Larionova, O. E. Rut, Sem. Sci. Techn. **10**, 1578 (1995).

[18] G. M. Minkov, A. V. Germanenko, V. A. Larionova, O. E. Rut, Phys. Rev. B**54**, 1841 (1996).

[19] J. Bardin, Phys. Rev. Lett. **6**, 57 (1961).

[20] Eric D. Siggia, and P. C. Kwok, Phys. Rev. B**2**, 1024 (1970).